Cell Stem Cell
Article

Loss of Fbw7 Reprograms Adult Pancreatic Ductal Cells into α, δ, and β Cells

Rocio Sancho,[1] Ralph Gruber,[1] Guoqiang Gu,[2] and Axel Behrens[1,3,*]
[1]Mammalian Genetics Laboratory, Cancer Research UK London Research Institute, Lincoln's Inn Fields Laboratories, 44, Lincoln's Inn Fields, London WC2A 3LY, UK
[2]Department of Cell and Developmental Biology, School of Medicine, Vanderbilt University, Nashville, TN 37232, USA
[3]School of Medicine, King's College London, Guy's Campus, London SE1 1UL, UK
*Correspondence: axel.behrens@cancer.org.uk
http://dx.doi.org/10.1016/j.stem.2014.06.019

SUMMARY

The adult pancreas is capable of limited regeneration after injury but has no defined stem cell population. The cell types and molecular signals that govern the production of new pancreatic tissue are not well understood. Here, we show that inactivation of the SCF-type E3 ubiquitin ligase substrate recognition component Fbw7 induces pancreatic ductal cells to reprogram into α, δ, and β cells. Loss of *Fbw7* stabilized the transcription factor Ngn3, a key regulator of endocrine cell differentiation. The induced β cells resemble islet β cells in morphology and histology, express genes essential for β cell function, and release insulin after glucose challenge. Thus, loss of *Fbw7* appears to reawaken an endocrine developmental differentiation program in adult pancreatic ductal cells. Our study highlights the plasticity of seemingly differentiated adult cells, identifies Fbw7 as a master regulator of cell fate decisions in the pancreas, and reveals adult pancreatic duct cells as a latent multipotent cell type.

INTRODUCTION

The pancreas comprises an exocrine component (ductal and acinar cells) and an endocrine component (β cells, α cells, δ cells, pancreatic polypeptide-positive [pp] cells, and ε cells). The endocrine cells are organized in defined islet structures embedded in the acinar compartment, which function as key regulators of carbohydrate metabolism (Edlund, 2002). The autoimmune disease Type 1 diabetes irreversibly destroys insulin-secreting β cells in pancreatic islets, resulting in a lack of insulin production and hyperglycemia (Atkinson et al., 2011). Treatment is most commonly with insulin injections, but the degree of glycemic control with this approach does not compare to functional pancreatic β cells. Regenerative β cell treatments in diabetic patients could allow for the long-term restoration of normal glycemic control and thus represent a potentially curative therapy (Yi et al., 2013).

The generation of new pancreatic β cells is being pursued on several fronts in vitro, including differentiation of induced pluripotent stem cells (iPSCs) and reprogramming of other pancreatic cell types (Pagliuca and Melton, 2013). Regenerating pancreatic β cells in situ is an attractive alternative to these approaches, driven by evidence of spontaneous β cell neogenesis in the adult pancreas (Bonner-Weir et al., 2004; Dor et al., 2004; Lysy et al., 2012; Pagliuca and Melton, 2013; Teta et al., 2005). β cell regeneration during adulthood is very limited but can be achieved experimentally using pancreatic duct ligation in mice (Xu et al., 2008) and pancreatectomy in rats (Bonner-Weir et al., 2004). Inducible depletion of acinar and islet cells with diphtheria toxin showed that duct cells can give rise to both acinar and endocrine cells (Criscimanna et al., 2011). Thus, ductal cells in the adult pancreas show a latent propensity for β cell generation. Additionally, genetic approaches have converted other pancreatic cell types into β cells. Adenoviral overexpression of the three transcription factors neurogenin-3 (Ngn3), Maf1a, and Pdx1 is sufficient to convert adult acinar cells into β cells (Zhou et al., 2008), and overexpression of *Pax4* converts glucagon-producing α cells into β cells (Collombat et al., 2009). However, the capacity for β cell neogenesis in the normal adult pancreas, and the regulatory events surrounding it, remain largely unknown.

Ngn3 is the earliest factor that specifically regulates the development of the endocrine compartment in the embryonic pancreas (Habener et al., 2005). *Ngn3*$^{-/-}$ mice completely lack endocrine islet development (Gradwohl et al., 2000), and transgenic overexpression of *Ngn3* activates an islet differentiation program in the embryo and in cultured pancreatic ductal cell lines (Heremans et al., 2002; Schwitzgebel et al., 2000). In the adult pancreas, *Ngn3* expression is very limited, but levels rise during β cell neogenesis induced by pancreatic duct ligation, where Ngn3 is required for β cell replenishment (Van de Casteele et al., 2013; Xu et al., 2008). Moreover, expansion of Ngn3+ cells bordering the ducts contributes to the β cell expansion observed when overexpressing Pax4 (Al-Hasani et al., 2013), indicating that manipulation of Ngn3 levels and/or activity may be beneficial for regeneration therapies. Ngn3 is a highly unstable protein (Roark et al., 2012), and the level and timing of its expression must be precisely controlled to ensure the correct production of β cells, but the details of its posttranslational regulation remain elusive.

Fbw7 (F-box and WD-40 domain protein 7) is the substrate recognition component of an evolutionarily conserved SCF

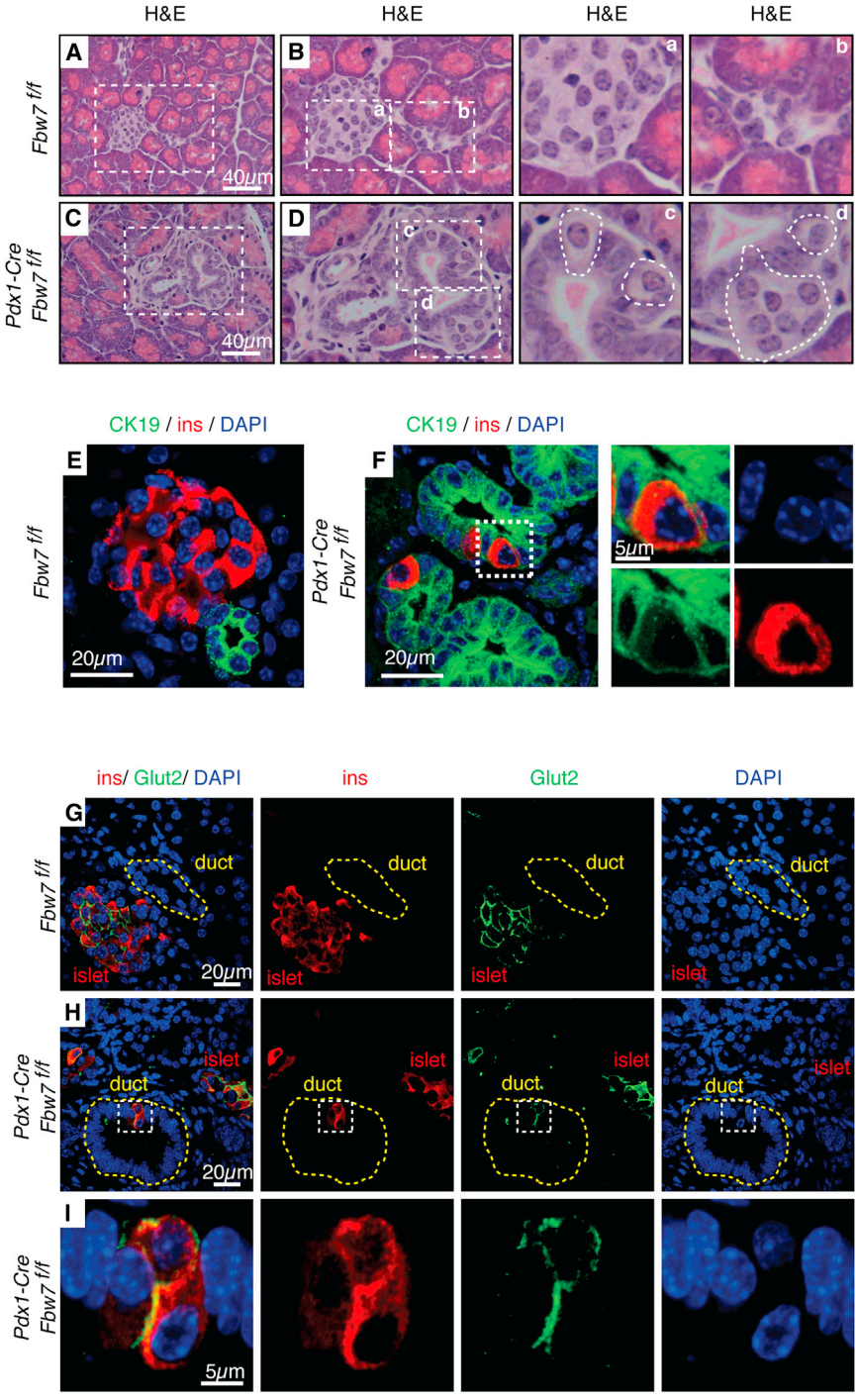

Figure 1. *Pdx1*-Driven Deletion of *Fbw7* in the Pancreas Induces Occurrence of Cells in the Ducts Displaying β Cell Hallmarks

(A–D) Hematoxylin and eosin (H&E) staining of *Fbw7*$^{f/f}$ or *Pdx1-Cre; Fbw7*$^{f/f}$ pancreas. (a) *Fbw7*$^{f/f}$ pancreatic islet; (b) *Fbw7*$^{f/f}$ duct; (c) and (d) *Pdx1-Cre; Fbw7*$^{f/f}$ cells with altered morphology in the ducts.

(E and F) Double IF for insulin (ins) and cytokeratin 19 (CK19) in *Fbw7*$^{f/f}$ (E) or *Pdx1-Cre; Fbw7*$^{f/f}$ (F) pancreas at 4 weeks.

(G–I) Double IF for Glut2 and insulin in *Fbw7*$^{f/f}$ (G) or *Pdx1-Cre; Fbw7*$^{f/f}$ (H and I) pancreas at 4 weeks. Nuclei were counterstained with DAPI. White dashed squares in (F) and (H) represent the areas magnified in (F) and (I) respectively. n > 5 mice per genotype (representative picture shown). See also Figure S1.

(complex of SKP1, CUL1, and F-box protein)-type ubiquitin ligase. SCF(Fbw7) degrades proteins that function in cellular growth and division pathways, including c-Myc, cyclin E, Notch, and c-Jun (Welcker and Clurman, 2008). Emerging evidence shows that Fbw7 controls stem cell self-renewal, cell fate decisions, survival, and multipotency in numerous tissues, including the hematopoietic (Iriuchishima et al., 2011) and nervous systems (Hoeck et al., 2010; Matsumoto et al., 2011), liver (Onoyama et al., 2011), and intestine (Sancho et al., 2010). This suggests that Fbw7 has a crucial function in fundamental cell differentiation processes.

Here, we show that Fbw7 contributes to the regulation of Ngn3 stability, and loss of *Fbw7* induces a direct ductal-to-β cell differentiation in the adult pancreas. Our study not only reveals a role for Fbw7 in pancreatic cell fate determination and identifies Ngn3 as a target of Fbw7 but also demonstrates that ductal cells can be induced to alter their identity in the adult pancreas in the absence of injury to the organ with a single genetic change.

RESULTS

Fbw7 Deletion in the Pancreas Induces Scattered Duct Cells to Display Functional Mature β Cell Hallmarks

Given the role of Fbw7 in controlling cell fate decisions in other organs, we asked whether Fbw7 also functions in cell type specification in the pancreas. We deleted *Fbw7* in embryonic pancreatic progenitor cells using a Cre recombinase under the control of the *Pdx1* promoter (*Pdx1-Cre; Fbw7*$^{f/f}$ mice). Although pancreatic organ size and gross morphology appeared normal, histological analysis revealed increased ductal cell proliferation and an expansion of the ductal compartment (Figures S1A and S1B available online), consistent with the increase in proliferation upon *Fbw7* deletion observed in other organs (Hoeck et al., 2010; Matsumoto et al., 2011; Onoyama et al., 2007, 2011; Sancho et al., 2010). Unexpectedly, scattered cells in the *Pdx1-Cre; Fbw7*$^{f/f}$ ducts showed an enlarged cytoplasm and smaller rounded nuclei when compared with surrounding ductal cells, and more closely resembled islet β cells (Figures 1A–1D). Insulin expression, which is normally

restricted to islets in control mice (Figure 1E), was detected in these aberrant ductal cells (Figure 1F). The majority of insulin-positive cells in *Pdx1-Cre; Fbw7$^{f/f}$* ducts were devoid of the ductal cell marker cytokeratin-19 (CK19), but costaining of CK19 and insulin was sometimes observed (Figure 1F), suggesting an intermediate transition state between ductal and insulin-positive cells. No insulin costaining with the acinar cell marker amylase was observed (Figures S1C and S1D). Thus, the absence of Fbw7 appears to trigger abnormal differentiation of a subset of ductal cells, biasing them toward an endocrine fate.

In addition to ectopic insulin-positive cells (in 17% of ducts), *Pdx1-Cre; Fbw7$^{f/f}$* ducts also contained cells expressing the α cell marker glucagon, albeit less frequently (3% of ducts) (Figures S1E and S1F). We also observed glucagon/insulin double-positive cells in *Pdx1-Cre; Fbw7$^{f/f}$* ducts (Figures S1G–S1I), similar to progenitor cells described in human embryonic pancreas (Piper et al., 2004). Thus, deletion of *Fbw7* in the pancreas promotes the occurrence of cells coexpressing markers of different pancreatic cell lineages, a cellular phenotype that is not normally observed in the adult pancreas.

One of the features of functional β cells is the expression of the glucose transporter Glut2 (*Slc2a2*). In control animals, Glut2 was coexpressed with insulin in islet β cells by double insulin/glut2 immunofluorescence (IF) (Figure 1G). Glut2 was also coexpressed with insulin in the *Pdx1-Cre; Fbw7$^{f/f}$* aberrant ductal cells (Figures 1H and 1I).

Inducible Deletion of *Fbw7* in the Adult Pancreas Promotes β Cell Neogenesis

Because Pdx1-expressing progenitors give rise to all the pancreatic lineages (Oliver-Krasinski and Stoffers, 2008), the emergence of insulin-positive cells in *Pdx1-Cre; Fbw7$^{f/f}$* ducts could be due to a developmental defect. To test whether *Fbw7* deletion can induce β cell neogenesis in adult mice, and to clarify the cells that give rise to ectopic β cells, we combined inducible *Fbw7* deletion using the *R26-CreERT* line with lineage tracing using *R26-LSL-YFP*. "*RY*" control mice express a tamoxifen-inducible form of Cre recombinase from the ubiquitous Rosa26 (R26) promoter, leading to the permanent expression of yellow fluorescent protein (YFP) in recombined cells. In the *Fbw7$^{f/f}$* background ("*RFY*" line, Figure 2A), tamoxifen treatment results in recombination of the floxed *Fbw7* alleles in Cre-expressing cells concomitantly with activation of YFP expression (Figure 2B).

Intraperitoneal injection of tamoxifen induced recombination in all pancreatic cell types but with different efficiencies. Almost all acinar cells showed YFP positivity (91%), while recombination occurred much less frequently in islet (10%) and ductal cells (5%) (Figures 2C and 2D). Despite the high percentage of recombination in the acinar compartment (Figure 2D), no insulin positivity was observed in cells with acinar cell morphology, and insulin/amylase double-positive cells could not be detected in the *RFY* pancreas (Figures 2E–2N). Likewise, direct intrapancreatic injection of 4-OH-tamoxifen into the pancreatic tail resulted in exclusive recombination in acinar cells, and here, no β cell neogenesis was observed (Figures S2A–S2D). In contrast, despite the low percentage of recombination in ducts (5%), *RFY* mice gave rise to insulin/green fluorescent protein (GFP) double-positive cells in ducts as early as 13 days postintraperitoneal injection of tamoxifen (Figures 2E–2N) as well as at later time points (Figures S2E and S2F). Therefore, *Fbw7* deletion in ductal cells, but not in acinar cells, induces the acquisition of β cell identity.

Deletion of *Fbw7* in the Pancreas Leads to Increased Ngn3 Protein Levels

Fbw7 targets many proteins involved in proliferation and differentiation for proteasomal degradation, such as N-terminally phosphorylated c-Jun (p-c-Jun^{Ser73}), Notch intracellular domain 1 (NICD1), phosphorylated c-Myc, and phosphorylated Cyclin E (Welcker and Clurman, 2008). It has been shown that SCF(Fbw7)-mediated substrate degradation is tissue specific (Hoeck et al., 2010; Ishikawa et al., 2008; Nakayama and Nakayama, 2006; Onoyama et al., 2007, 2011; Sancho et al., 2010; Thompson et al., 2008; Wang et al., 2012). Western blotting of lysates from whole *Pdx1-Cre; Fbw7$^{f/f}$* pancreas, in which *Fbw7* is inactivated in all pancreatic cell types, showed increased p-c-Jun^{Ser73} and NICD1 protein levels when compared to *Fbw7$^{f/f}$* controls, while phosphorylated c-Myc and Cyclin E levels were not substantially affected (Figure 3A; quantifications in Figures S3A and S3B). In β cells, NICD1 and p-c-Jun^{Ser73} were barely detectable, either in control *RY* or in *Fbw7*-deleted *RFY* pancreas (Figure S3C). In the acinar compartment, the loss of *Fbw7* did not increase p-c-Jun^{Ser73} or NICD1 in *RFY* compared with *RY* mice (Figure S3D). In order to analyze Fbw7 function in ducts, we examined sections from *Pdx1-Cre; Fbw7$^{f/f}$* animals. p-c-Jun^{Ser73} fluorescence intensity was increased in *Pdx1-Cre; Fbw7$^{f/f}$* compared with control ducts (Figures 3B and 3C), suggesting that SCF(Fbw7) primarily acts in pancreatic ductal cells.

Of the known substrates increased by *Fbw7* loss in the pancreas, none are thought to be involved in β cell neogenesis. While Notch has been reported to be involved in embryonic pancreatic differentiation, it has been proposed to inhibit β cell neogenesis rather than promoting it (Esni et al., 2004; Murtaugh et al., 2003). We therefore examined the possibility that Fbw7 in the pancreas may control the levels of one or more other substrates. Transcription factors involved in embryonic β cell development include Pdx1, Ngn3, Hnf3, and Hnf6 (Zaret, 2008). Pdx1, Hnf3, and Hnf6 protein levels were unaltered in *Pdx1-Cre; Fbw7$^{f/f}$* compared with *Fbw7$^{f/f}$* pancreas, but the protein levels of Ngn3 were strongly increased (Figure 3D; quantifications in Figures S3E and S3F). *Ngn3* messenger RNA (mRNA) levels were also increased (Figure 3E), in agreement with previous reports of positive autoregulatory loops controlling *Ngn3* expression (Ejarque et al., 2013; Wang et al., 2008). The increase in Ngn3 after *Fbw7* loss also correlated with higher mRNA levels of the Ngn3 transcriptional target genes *Insm1*, *HeyL*, *Ctgf*, and *Nkx2-2* (Swales et al., 2012) when analyzed by quantitative PCR (qPCR) (Figure 3E), and increased protein levels of the Ngn3 transcriptional targets NeuroD1 and Insm1 (Figures 3D, 3F, 3G, S3E, and S3F). Ngn3 is a key regulator of endocrine differentiation, making it an excellent candidate for inducing β cell neogenesis induced by *Fbw7* loss.

Fbw7 Binds to, Ubiquitinates, and Induces Proteasomal Degradation of Ngn3

To investigate the mechanism by which Fbw7 affects Ngn3, we first analyzed the stability of Ngn3 protein using cycloheximide to inhibit protein synthesis. Ngn3 half-life was increased more than

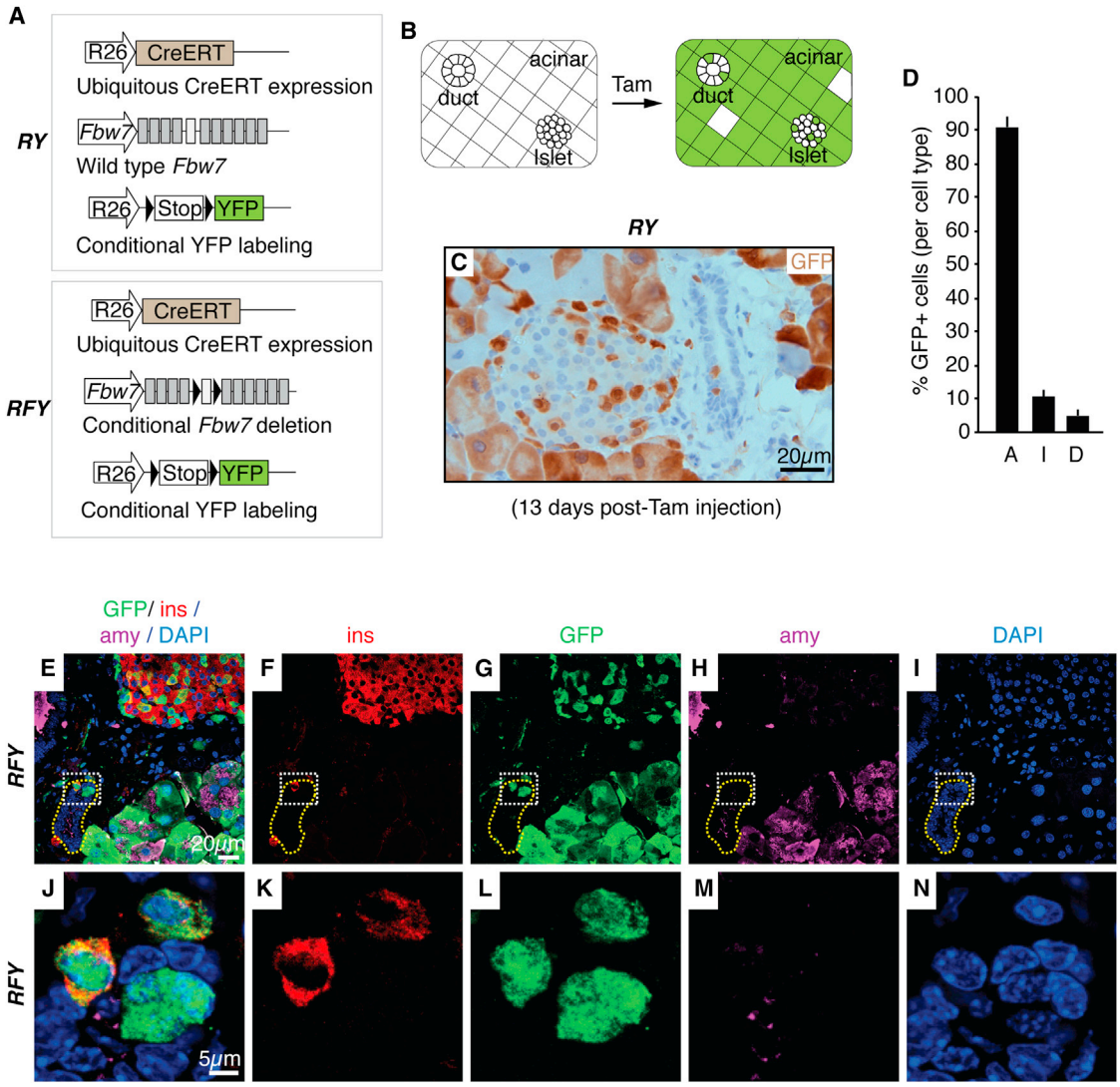

Figure 2. Inducible Deletion of *Fbw7* in the Adult Pancreas Promotes β Cell Neogenesis

(A) Scheme of the *RY (R26-CreERT; R26-LSL-YFP)* and *RFY (R26-CreERT; Fbw7$^{f/f}$; R26-LSL-YFP)* mouse models.

(B) Schematic diagram of *RY* pancreas before and after tamoxifen (Tam) injection.

(C) GFP immunoperoxidase staining in *RY* pancreas after tamoxifen injection. Section shows acinar cells, an islet, and a duct. n > 3 mice per genotype.

(D) Quantification of GFP-positive cells in the different pancreatic cell type compartments of *RY* (n = 3) mice 13 days postinjection. A, acinar; I, islet; D, ducts. Data are represented as mean + SEM.

(E–N) Triple IF for insulin (ins), GFP, and amylase (amy) in *RFY* mice 13 days after tamoxifen injection. n > 3 mice per genotype. Nuclei were counterstained with DAPI. Ducts are circled with a yellow dashed line. White dashed squares represent the area magnified in the squares shown below.

See also Figure S2.

2-fold after *Fbw7* silencing, suggesting that Fbw7 acts to destabilize Ngn3 protein (Figure 4A). Ngn3-hemagglutinin (Ngn3-HA) coimmunoprecipitated Flag-tagged Fbw7 isoform-α and, to a lesser extent, isoform-β (Figure 4B, left panel; and vice versa, as shown in the right panel), and endogenous Fbw7 interacted with Ngn3-HA (Figure 4C). Ngn3 is a heavily ubiquitinated protein (Roark et al., 2012), but Ngn3 ubiquitination was strongly reduced in *Fbw7*$^{\Delta}$ HCT116 cells when compared to congenic *Fbw7*^{wt} cells (Figure 4D). In vitro, wild-type (WT) Fbw7–Flag protein complexes promoted efficient ubiquitination of recombinant Ngn3, but the inactive mutant Fbw7α-ΔFbox–Flag did not (Welcker et al., 2004) (Figures 4E and S4A). All together, these data suggest that Ngn3 is a substrate of the SCF(Fbw7) ubiquitin ligase.

Most Fbw7 substrates contain a phosphodegron motif that serves as the recognition motif for Fbw7 interaction (Welcker and Clurman, 2008). Multiple higher molecular weight bands of Ngn3-HA detected by immunoblot collapsed after calf intestinal phosphatase (CIP) treatment, suggesting that they represent phosphorylated forms. Silencing of *Fbw7* increased the levels of these higher molecular weight forms (Figure 4F). GSK3β is the kinase responsible for modifying the phosphodegron motifs

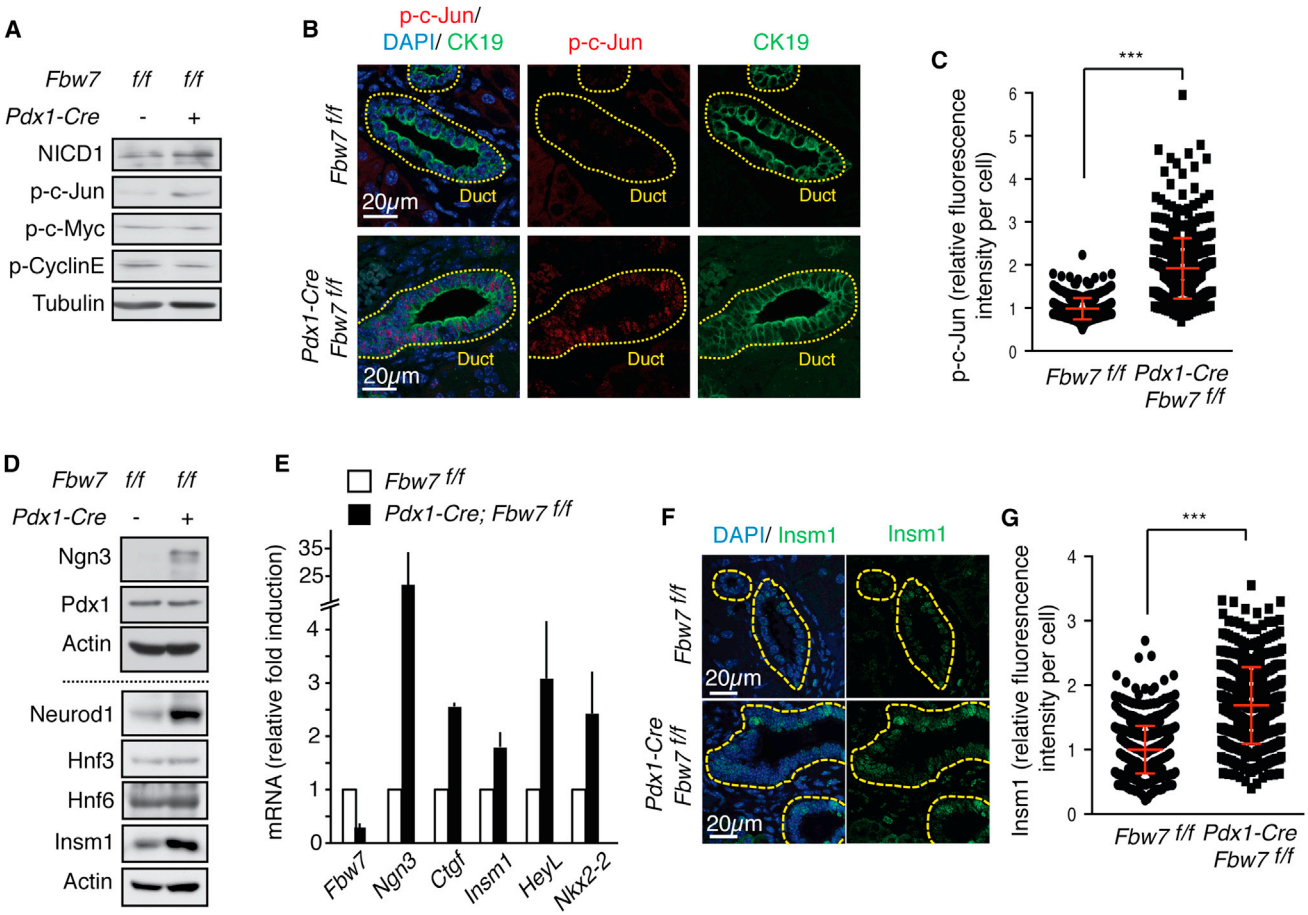

Figure 3. *Fbw7* Loss in the Pancreas Leads to Increased Ngn3 Protein Levels

(A–D) In (A) and (D), a western blot analysis is shown of $Fbw7^{f/f}$ and *Pdx1-Cre; Fbw7*$^{f/f}$ whole pancreas lysates. n = 3 mice per genotype. (B) Double IF of CK19 and p-c-Jun^{Ser73} in $Fbw7^{f/f}$ and *Pdx1-Cre; Fbw7*$^{f/f}$ pancreas at 4 weeks. n > 3 mice per genotype (representative picture shown). (C) Quantification of experiment in (B). p-c-Jun fluorescence intensity was measured using LSM software; each dot represents the mean intensity of a single cell. $Fbw7^{f/f}$ n = 471 cells (20 ducts/2 mice); *Pdx1-Cre; Fbw7*$^{f/f}$ n = 505 cells (20 ducts/3 mice).

(E) qPCR analysis of Ngn3 target genes from $Fbw7^{f/f}$ and *Pdx1-Cre; Fbw7*$^{f/f}$ mouse pancreas at 4 weeks. n > 3 mice per genotype. Error bars indicate SEM.

(F) IF for Insm1 in $Fbw7^{f/f}$ and *Pdx1-Cre; Fbw7*$^{f/f}$ pancreas at 4 weeks. Ducts are circled with a yellow dashed line.

(G) Quantification of experiment in (F). Insm1 fluorescence intensity per cell was measured as for p-c-Jun above. $Fbw7^{f/f}$ n = 518 cells (20 ducts/2 mice); *Pdx1-Cre; Fbw7*$^{f/f}$ n = 527 cells (20 ducts/3 mice).

Error bars in (C) and (G) represent mean ± SD. See also Figure S3 and Table S1.

of c-Myc and Notch1 (Welcker and Clurman, 2008; Welcker et al., 2004). In silico analysis revealed a GSK3β consensus site at the Ngn3 C terminus (Ser183–Ser187). GSK3β inhibitor treatment increased Ngn3 protein levels (Figure 4G), suggesting that GSK3β regulates the stability of Ngn3. We generated constructs of Ngn3 with Ser183 and/or Ser187 mutated to alanine to assess the role of the putative phosphodegron motif (Figure 4H). Mutation of the predicted GSK3β phosphorylation site Ser183 altered the electrophoretic mobility of Ngn3 protein, while mutation of Ser187 had less effect (Figure 4I, left panel). While WT Ngn3 could efficiently interact with Fbw7, the interaction was severely impaired when Ser183 was mutated (Ngn3-AA and Ngn3-AS; Figure 4I, right panel). Accordingly, while the mRNA levels from all four Ngn3 constructs were comparable, the stability of Ngn3-AA and Ngn3-AS was greatly increased (Figures S4B and S4J). These data suggest that Fbw7 directly controls Ngn3 stability by regulating its ubiquitination and proteasomal degradation and that GSK3β-mediated phosphorylation of Ser183 might regulate this process. Since Ngn3 has been shown to be involved in β cell neogenesis in the adult pancreas (Al-Hasani et al., 2013; Baeyens et al., 2006; Xu et al., 2008), accumulation of Ngn3 protein is likely to contribute to adult β cell neogenesis induced by *Fbw7* inactivation.

Conditional Overexpression of Ngn3-AA in the Adult Pancreatic Ducts Induces β Cell Neogenesis

To determine whether accumulation of Ngn3 protein is sufficient to induce β cell neogenesis, we generated a conditional inducible transgenic mouse line that expresses the phospho mutant, stable form of Ngn3 (Ngn3-AA) together with GFP after Cre recombination (*Pdx1-Cre*; Rosa26-*loxSTOPlox-Ngn3-AA-IRES-GFP* or *Pdx1-Cre*; *R26-LSL-Ngn3-AA*; Figure 5A). *Pdx-Cre*

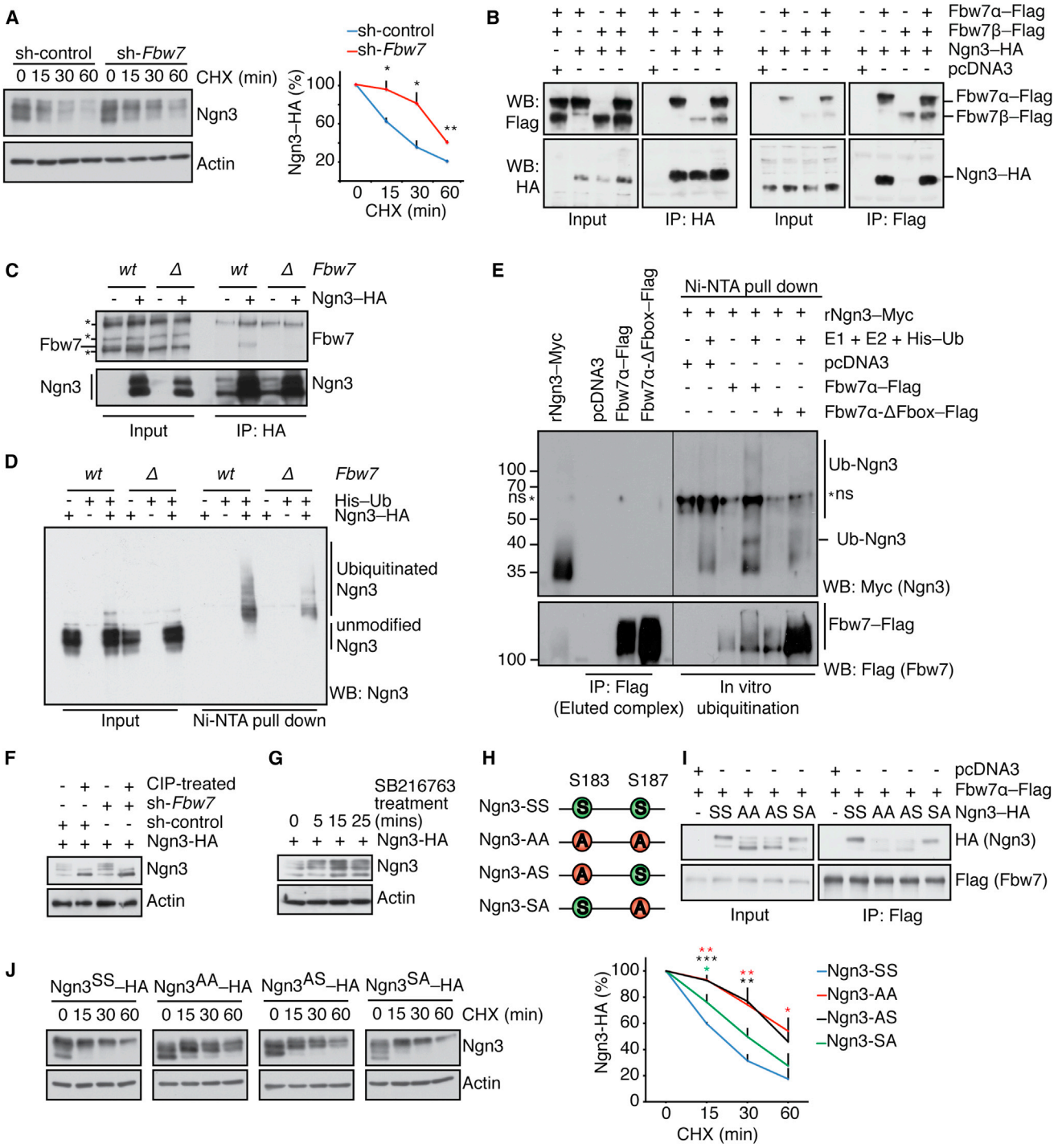

Figure 4. Fbw7 Binds to and Ubiquitinates Ngn3 and Induces Its Proteasomal Degradation

(A) Western blot analysis of Ngn3 protein levels during a cycloheximide (CHX) time course after silencing *Fbw7*. Graph shows mean Ngn3 levels normalized to actin, as a percentage of initial protein levels. n = 3 independent experiments.

(B) Ngn3–HA and Fbw7α–Flag/Fbw7β–Flag IP from cotransfected HEK293T cells. Western blots (WB) of input and IP material are shown.

(C) HA IP from HCT116-*Fbw7*^{wt} and *Fbw7* knockout (*Fbw7*^{Δ}) cells transfected with Ngn3-HA. Anti-Fbw7 (Bethyl Laboratories) detects endogenous Fbw7.

(D) In vivo Ngn3 ubiquitination is reduced in *Fbw7*^{Δ} compared with *Fbw7*^{wt} cells. Ubiquitinated Ngn3 was resolved by Ni^{2+}-NTA affinity purification and immunoblotting with anti-Ngn3 antibody.

(E) Recombinant Ngn3 (rNgn3-myc) is ubiquitinated in vitro, using Flag-IP complexes of pcDNA3, Fbw7α-Flag, or Fbw7α-ΔFbox-Flag from transfected HEK293T cells. Ubiquitinated complexes were enriched by Ni^{2+}-NTA affinity purification before immunoblotting.

(F) Calf intestinal phosphatase (CIP) treatment of lysates from Ngn3-HA and sh-control/sh-*Fbw7* cotransfected HEK293T cells.

(legend continued on next page)

induced recombination in mouse pancreas but not in liver or tail (Figure 5B). Ngn3 protein, which is undetectable in control adult pancreas, was detected in *Pdx1-Cre; R26-LSL-Ngn3-AA* pancreas (Figure 5C) but not in liver. *Pdx1-Cre; R26-LSL-Ngn3-AA* pancreas showed increased *Ngn3* and *Ins2* mRNA levels when compared to unrecombined *R26-LSL-Ngn3-AA* mice (Figure 5D). Transgenic Ngn3-AA expression resulted in increased β cell area as analyzed by immunostaining for insulin (Figures 5E and 5F). These data suggested that the overexpression of a stable form of Ngn3 (Ngn3-AA) from embryonic pancreas development onward results in an increase in β cells. In order to test whether overexpression of Ngn3-AA in the adult pancreatic ducts was sufficient to induce β cell reprogramming, we crossed *R26-LSL-Ngn3-AA* mice to *CK19-CreERT* mice, in which the expression of tamoxifen-inducible Cre-ERT protein is driven by the promoter of the ductal marker cytokeratin 19 (Means et al., 2008) (Figure 5G). Thirteen days post-tamoxifen injection (Figure 5H), GFP expression could be detected specifically in ductal cells of *CK19-CreERT; R26-LSL-Ngn3-AA* mice, while it was absent in *R26-LSL-Ngn3-AA* ducts (Figure 5I). Furthermore, we detected a significant increase in insulin-positive ductal cells in tamoxifen-injected *CK19-CreERT; R26-LSL-Ngn3-AA* pancreas (Figures 5J and 5K), suggesting that Ngn3-AA overexpression in the adult pancreatic duct is sufficient to induce ductal-to-β cell conversion.

Fbw7 Deletion in the Adult Pancreatic Ducts Induces Direct Conversion of Ductal Cells into β Cells

The aforementioned data suggest that Fbw7 may control adult β cell neogenesis by regulating Ngn3 protein stability. To test whether β cells arise as a direct consequence of *Fbw7* loss in ductal cells, we asked whether loss of *Fbw7*, specifically in the adult ductal compartment, is sufficient to achieve cell conversion. To this end, we generated *CK19-CreERT; Fbw7*$^{+/+}$*; R26-LSL-YFP* ("*CY*") control and *CK19-CreERT; Fbw7*$^{f/f}$*; R26-LSL-YFP* ("*CFY*") inducible *Fbw7* deletion mice (Figures 6A and 6B). The efficiency of recombination 2 weeks after tamoxifen injection was between 40% and 50% in both *CY* and *CFY* ducts, as reported previously (Means et al., 2008). Complete recombination was confirmed by PCR analysis of genomic DNA isolated from YFP+ *CFY* cells (Figure 6C). qPCR analysis demonstrated that *Fbw7* mRNA was highly expressed in *CY* ductal cells but undetectable in *CFY* ductal cells and mature pancreatic β-cells sorted from *MIP-GFP* mice (in which GFP expression is driven by the insulin promoter) (Figure 6D). These data suggest that *Fbw7* mRNA is enriched in ductal cells, in agreement with substrate stabilization predominantly in this cell type after *Fbw7* loss (Figure 3B).

Fbw7 inactivation in ductal cells did not alter the number of ducts (Figure 6E) or islets (Figure 6F). However, a significant number of insulin-positive cells (almost 0.5%, i.e. ~1% of the *Fbw7* knockout cells if considering ~50% recombination efficiency) was observed in the ducts of *CFY* mice, while they rarely arose in *CY* mice (Figure 6G). About 12% of the *CFY* ducts contained induced β cells, typically between one and three cells per duct. It is interesting that 3.8% of *CFY* ducts contained glucagon-positive α cells and 5.5% contained somatostatin-positive δ cells, while pp or amylase-positive ductal cells were never detected (Figures S4C and S4D). Thus, deletion of *Fbw7* in adult pancreatic ductal cells induces conversion of some ductal cells to α or δ cells or, most frequently, to β cells.

Inactivation of *Fbw7* could trigger resident ductal progenitor cell proliferation followed by redifferentiation or induce direct transdifferentiation. To distinguish between these possibilities, *Fbw7* inactivation and lineage tracing was combined with long-term bromodeoxyuridine (BrdU) labeling. BrdU was incorporated in scattered cells in the pancreatic *CY* ducts and increased in *CFY* ducts (Figures 6H, 6I, and S4E). However, less than 1% of insulin-positive *CFY* duct cells were labeled after 2 weeks of continuous BrdU exposure, beginning directly before *Fbw7* deletion (Figures 6J, S4F, and S4G). Thus *Fbw7* deletion in the adult pancreatic ducts induces direct conversion of a subset of exocrine ductal cells into endocrine β cells, without a requirement for cell proliferation.

Induced β Cells in Adult *Fbw7* Mutant Ducts Resemble Functional β Cells

To explore the functionality of the β cells formed after *Fbw7* deletion, we performed mRNA expression profiling of GFP+ sorted cells from tamoxifen-injected *CY* and *CFY* mice and compared them to GFP+ cells from *MIP-GFP* mice as a positive control for β cells (Figure 7A). *CFY* GFP+ ductal cells showed a modest increase in expression of numerous β cell specific genes, consistent with a small subset of ductal cells undergoing β cell conversion. In agreement with the increase in Ngn3 stability in *Fbw7*-deleted cells, *CFY* GFP+ ductal cells also showed an increase in the expression of reported Ngn3 target genes (*Chga*, *Insm1*, *Dll3*, *Syp*, *Chn1*, *HeyL*, *Atp2a3*, and *Pcsk2*; Swales et al., 2012) (Figure 7B). qPCR analysis confirmed increased mRNA expression of the β cell marker genes *Ins2*, *Gck*, *Pdx1*, and *Nkx6.1* in *CFY* GFP+ ductal cells compared with *CY* GFP+ cells (Figure 7C).

As well as showing gene expression characteristics of islet β cells, insulin-positive cells in the ducts of *CFY* mice costained with the functional β cell markers c-PPT, Glut2, MafA1, Nkx6.1, Pax6, PC1/3, Pdx1, Urocortin 3 (Ucn3), and Isl1, showing comparable staining to islet β cells (Figures 7D, 7E, and S5). Insulin-positive *CFY* ductal cells were negative for the ductal markers Sox9 and DBA, while other *CFY* ductal cells retained expression of these markers (Figures 7E and S5).

An important hallmark of β cell function is the ability to release insulin after glucose stimulation. To test this, we

(G) GSK3β inhibitor (SB216763) treatment of cells transfected with Ngn3-HA.
(H) Graphic scheme of *Ngn3* mutant constructs generated, showing the putative GSK3β phosphorylation site in mouse Ngn3. S, serine; A, alanine.
(I) Ser183Ala mutation (AA, AS) disrupts Ngn3 interaction with Fbw7. Left: input. Right: Fbw7α-Flag IP from HEK293T cells co-transfected with Ngn3–HA or the indicated mutant construct.
(J) Ser183Ala mutation (AA, AS) increases Ngn3 stability. Ngn3 protein levels were measured after cycloheximide treatment in cells transfected with different Ngn3–HA mutants. Graph shows mean Ngn3 levels normalized to actin, as a percentage of initial protein levels.
In (B)–(I), n > 2 independent experiments. Error bars in (A) and (J) represent SEM; n = 3 independent experiments. See also Figure S4 and Table S1.

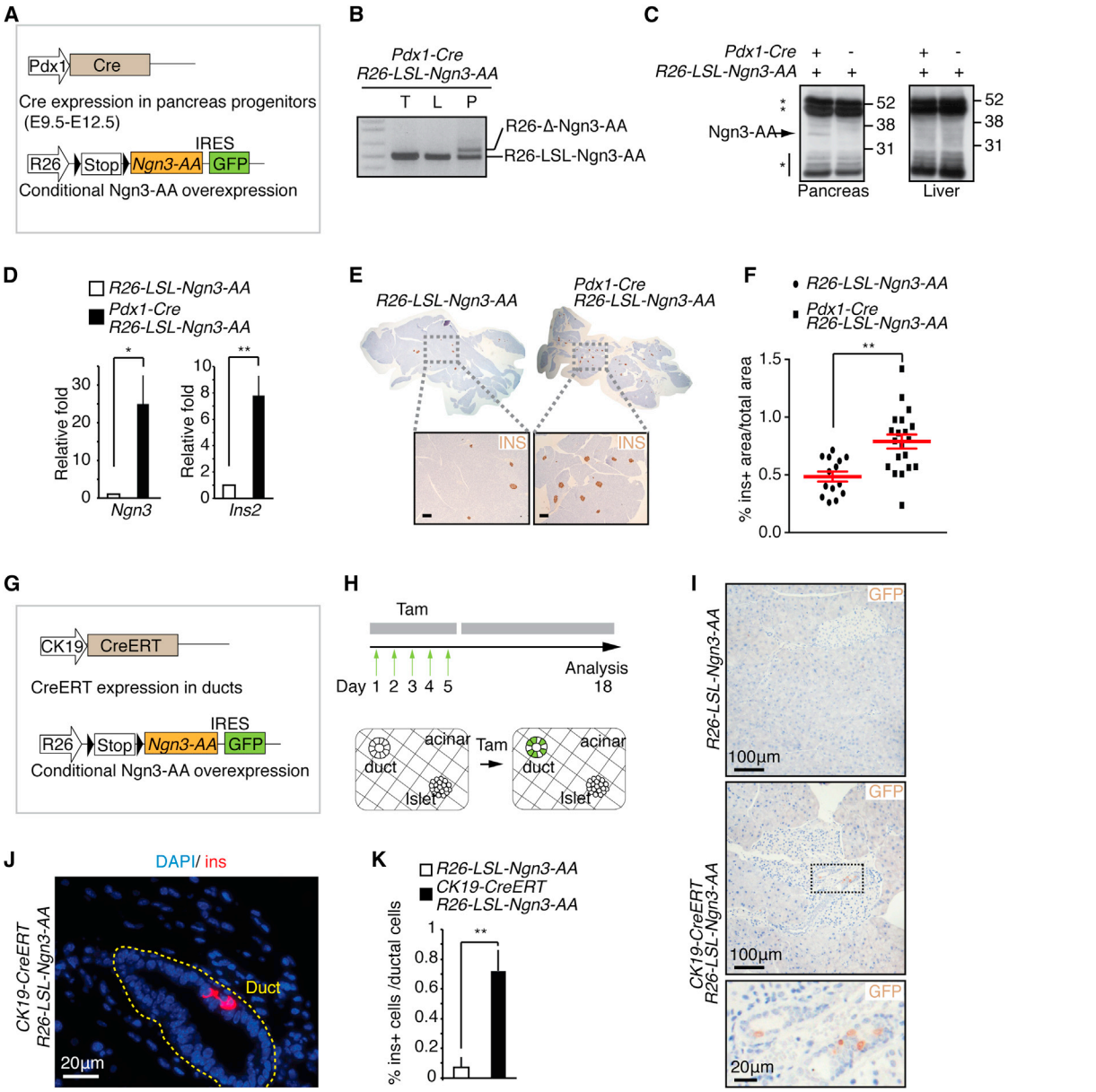

Figure 5. Conditional Overexpression of Ngn3-AA in the Adult Pancreatic Ducts Is Sufficient to Induce β Cell Neogenesis

(A) Schematic representation of the *Pdx1-Cre; R26-LSL-Ngn3-AA* model.

(B) *R26-LSL-Ngn3-AA* recombination PCR performed in genomic DNA from tail (T), liver (L) and pancreas (P).

(C) Western blot analysis for Ngn3 in *R26-LSL-Ngn3-AA* or *Pdx1-Cre; R26-LSL-Ngn3-AA* mouse pancreas and liver.

(D) qPCR analysis of *Ngn3* and *Ins2* in *R26-LSL-Ngn3-AA* or *Pdx1-Cre; R26-LSL-Ngn3-AA* pancreas. n = 3 mice per genotype. Error bars indicate SEM.

(E) Insulin staining in *R26-LSL-Ngn3-AA* or *Pdx1-Cre; R26-LSL-Ngn3-AA* mouse pancreas. Scale bar, 300 μm.

(F) Quantification of insulin-positive (ins+) area in *R26-LSL-Ngn3-AA* (n = 14 sections; 578 islets/3 mice) or *Pdx1-Cre; R26-LSL-Ngn3-AA* (n = 20 sections; 900 islets/4 mice). Dots represent percentage of ins+ cells for each section. Error bars represent mean ± SEM.

(G) Scheme of the *CK19-CreERT; R26-LSL-Ngn3-AA* model.

(H) Schematic diagram of the *CK19-CreERT; R26-LSL-Ngn3-AA* pancreas before and after tamoxifen injection.

(I) GFP immunoperoxidase staining in *R26-LSL-Ngn3-AA* or *CK19-CreERT; R26-LSL-Ngn3-AA* pancreas after tamoxifen injection. Dashed square indicates the area magnified.

(J) Representative picture showing insulin-positive cells in the pancreatic duct of tamoxifen-injected *CK19-CreERT; R26-LSL-Ngn3-AA* mice.

In (I) and (J), n > 5 mice per genotype (representative picture shown).

(K) Quantification of insulin-positive ductal cells in tamoxifen-injected *R26-LSL-Ngn3-AA* (n = 5 mice/3,462 cells) and *CK19-CreERT; R26-LSL-Ngn3-AA* animals (n = 8 mice/5,965 cells). Data are represented as mean + SEM.

See also Table S1.

subjected GFP+ cells sorted from *CY* and *CFY* mouse pancreas to in vitro glucose challenge (Figures 7F and 7G). While *CY* GFP+ cells did not respond to glucose, *CFY* GFP+ cells showed a substantial release of insulin (Figure 7G). Each *CFY* well of 30,000 cells contained approximately 300 converted β cells (based on a 1% conversion frequency), which secreted 214 pg (1.07 ng/ml) of insulin, i.e., 0.71 pg per cell. By comparison, 5,000 islet β cells sorted from a *MIP-GFP* pancreas responded to glucose by releasing 3,378 pg (16.89 ng/ml) of insulin, i.e., 0.67 pg per cell (Figure 7H). Based on this result, the response to glucose challenge in the converted cells is comparable to that of islet β cells (Figure 7I). Thus, the β cells converted after *Fbw7* loss in the adult pancreatic ducts show both the characteristic marker expression and functionality of mature β cells.

DISCUSSION

Ectopic expression of combinations of transcription factors can induce changes of cellular fate in adult pancreatic tissue (Zhou et al., 2008); however, examples of reprogramming in vivo by loss of a single molecule are rare. In this study we show that Fbw7 maintains adult ductal cell fate, as *Fbw7* inactivation results in transdifferentiation of ductal cells into α and δ cells and, predominantly, β cells. The newly formed β cells resemble islet β cells with regard to cellular morphology, marker gene expression, and insulin secretion in response to glucose challenge. Our findings indicate an unexpected plasticity of ductal cells, in which loss of a single gene (*Fbw7*) renders the duct cells multipotent, able to remain exocrine or transdifferentiate into endocrine α, δ, or β cell types.

Fbw7 Function in the Adult Pancreas

Fbw7 is a key regulator of stem cell function, as *Fbw7* inactivation results in increased proliferation and impaired differentiation of hematopoietic, liver, intestinal, and neural progenitor cells (Hoeck et al., 2010; Iriuchishima et al., 2011; Matsumoto et al., 2011; Onoyama et al., 2011; Sancho et al., 2010, 2013). The potent tumor suppressor function of Fbw7 is likely to be a direct consequence of deregulated stem cell proliferation and differentiation (Wang et al., 2012). However, the role of Fbw7 in the pancreatic ducts is distinct from Fbw7 function in other organ systems. Ductal to endocrine cell transdifferentiation after *Fbw7* loss occurs in the absence of proliferation, suggesting that the subset of cells that respond to *Fbw7* deletion in this way does not behave as adult stem cells in other organ systems, requiring cell division before differentiation. Rather, Fbw7 seems to function in the adult pancreas to constantly maintain cell fate in a subset of ductal cells.

Fbw7 Loss Converts Adult Ductal Cells into Functional β Cells

We found that the expression and activity of Fbw7 in the adult pancreas is enriched in the ductal compartment. Adult pancreatic ducts have been suggested to harbor β cell progenitors, which are reactivated after challenge (Bonner-Weir et al., 2008). Pancreatic duct ligation (PDL), combined with lineage tracing of the ductal epithelium, demonstrated that a quarter of new β cells formed in response to injury were derived from ductal cells (Inada et al., 2008). In contrast, alloxan treatment was recently shown to induce transdifferentiation of acinar cells into β cells (Baeyens et al., 2014). We found that *Fbw7* expression was quickly and dramatically downregulated 24 hr after PDL, but alloxan treatment induced no change in *Fbw7* expression (Figures S6A and S6B). These data suggest that *Fbw7* transcriptional downregulation may contribute to duct-derived β cell neogenesis in response to pancreatic injury (Figure S6C).

Although it is conceivable that β cells produced elsewhere could migrate to the ducts, the location of induced β cells embedded within the ducts suggests that they originated in this compartment. Several lines of evidence support this interpretation: first, "transition" cells coexpressing ductal cell (CK19) and β cell (ins) markers are observed after *Fbw7* loss; second, genetic models in which recombination is inefficient in ducts (such as *RFY* mice injected intrapancreatically with OH-tamoxifen) do not induce β cell neogenesis; and third, duct-specific *Fbw7* loss combined with lineage tracing (our *CFY* model) induces the occurrence of ductal YFP-labeled insulin-positive cells.

Insulin-positive cells are also observed in ducts of normal unchallenged mice, albeit rarely (Teta et al., 2005), a finding we confirmed in this study. It is not known whether this spontaneous transdifferentiation process is similar to the reprogramming induced by *Fbw7* inactivation. However, bihormonal insulin/glucagon double-positive cells—presumptive α and β cell precursors during embryonic pancreas development (De Krijger et al., 1992) that we also observed in *Fbw7* deleted ducts—have not been described in unchallenged adult WT pancreas. Similarly, CK19/insulin transdifferentiation intermediates have not been reported in normal mice. Thus, β cell reprogramming induced by *Fbw7* inactivation appears to be a distinct process from the spontaneous appearance of insulin-positive cells in WT pancreatic ducts and may represent a reawakening of a multipotent state.

A frequent stumbling block in previous models inducing cell reprogramming has been the functionality of the newly formed β cells. It is important to note that *Fbw7*-mutant induced β cells secrete comparable amounts of insulin after glucose challenge as bona fide β cells isolated from *MIP-GFP* mice. Therefore, *Fbw7* loss appears to trigger the conversion of adult pancreatic ductal cells into apparently functional β cells.

The Fbw7-Ngn3 Axis as a Mechanism Regulating Adult β Cell Neogenesis

The activity of Fbw7 toward different substrates is tissue specific, and our results show that, in the pancreas, c-Jun, Notch, and Ngn3 levels are increased after *Fbw7* deletion. While c-Jun has no reported function in pancreatic cell fate decisions, the Notch signaling pathway is thought to inhibit pancreatic endocrine development (Apelqvist et al., 1999; Fujikura et al., 2006; Jensen et al., 2000; Oka et al., 1995). In contrast, we find that endocrine differentiation in the ducts after *Fbw7* deletion is accompanied by an increase in NICD1 levels. This could imply that Notch has different roles in embryonic and adult pancreatic β cell differentiation, but it is also possible that increased Notch signaling is not required for β cell neogenesis after *Fbw7* loss, and β cell neogenesis is induced despite an overall increase in Notch levels.

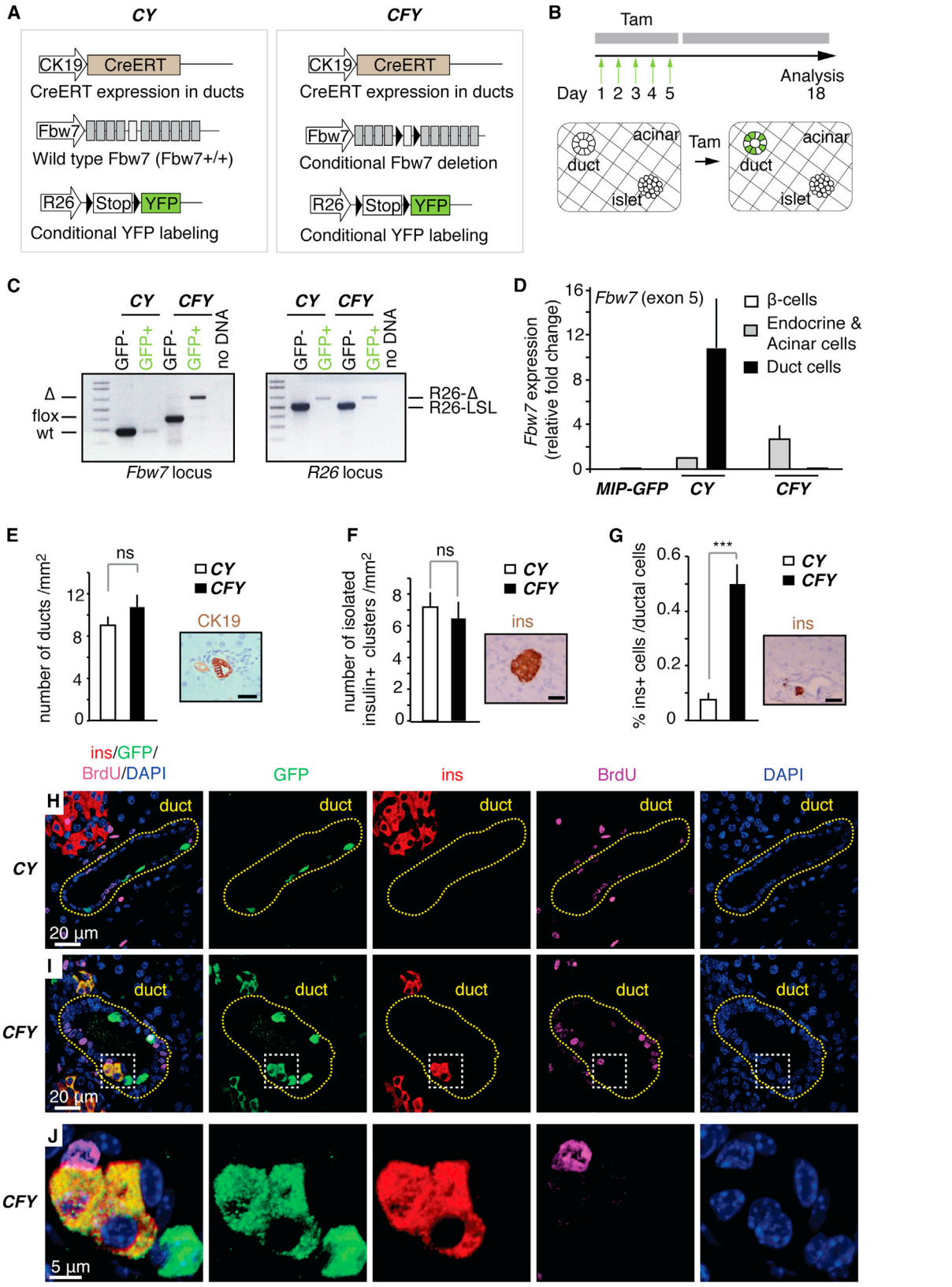

(legend on next page)

The stabilization of Ngn3 after *Fbw7* loss is consistent with a strong proendocrine signal. Ngn3 has been previously reported to be required for PDL- and *Pax4* overexpression-induced β cell neogenesis (Al-Hasani et al., 2013; Xu et al., 2008), and our data show that Ngn3 stabilization in the ducts is sufficient to induce β cell neogenesis (Figure 5). Despite its essential role in endocrine differentiation, and the reported Ngn3 instability at the protein level, the regulatory mechanisms that control the abundance of Ngn3 are not fully understood. In this study, we show that Ngn3 is a substrate for SCF(Fbw7). Ngn3 behaves as a canonical Fbw7 substrate, containing a GSK3 consensus phosphorylation site that, when mutated, increases the stability of the protein. Our data indicate that Ngn3 stabilization after *Fbw7* loss contributes to a transdifferentiation program, inducing ductal cells to differentiate into β cells. Induction of adult β cell neogenesis is desirable for diabetes treatment, and modulation of the Fbw7-Ngn3 axis could potentially be exploited as a therapeutic approach toward generation of new β cells for cell replacement therapies.

EXPERIMENTAL PROCEDURES

Mouse Lines

The *Pdx1-Cre* (Hingorani et al., 2003), *R26-LSL-YFP* (Srinivas et al., 2001), *CK19-CreERT* (Means et al., 2008), *R26-CreERT* (Ventura et al., 2007), *MIP-GFP* (Hara et al., 2003), and *Fbw7*$^{f/f}$ (Jandke et al., 2011) mouse lines have been previously described. The *R26-LSL-Ngn3-AA* mouse was generated using mouse *Ngn3-AA* complementary DNA (cDNA) to create a conditional *Rosa26-Ngn3-AA-IRES-eGFP-pA*$^{+}$ targeting vector as described elsewhere (Nyabi et al., 2009), followed by selection of embryonic stem cell clones targeted with linearized vector and generation of chimeric Swiss diploid embryos. All animal experiments were approved by the CRUK London Research Institute Animal Ethics Committee and conformed with UK Home Office regulations under the Animals (Scientific Procedures) Act 1986 including Amendment Regulations 2012.

Cell Lines and Plasmids

HCT116-*Fbw7*^{wt} and HCT116-*Fbw7*$^{\Delta}$ cells, and Fbw7α–Flag and Fbw7β–Flag constructs, have been described elsewhere (Grim et al., 2008). Full-length *Ngn3* cDNA from mouse embryonic pancreas was obtained by PCR and cloned into pcDNA3 to generate the pcDNA3-Ngn3 plasmid. Mutation of *Ngn3* Ser183/Ser187 to alanine was achieved by conventional PCR site-directed mutagenesis. p-RS-sh-control and p-RS-sh-Fbw7 constructs were generated by cloning short hairpin-containing oligos into the pRS vector (Addgene).

Genetic Labeling Experiments

For all experiments, adult (6–9 weeks except where indicated) age- and strain-matched animals were used. Mice were either injected intraperitoneally with 100 μg/g body weight of tamoxifen dissolved in peanut oil (at least three mice per genotype) or intrapancreatically injected with 20 μl–50 μM 4-OH-tamoxifen (two mice per genotype) as indicated. Analyses were performed 5/13 days (short term) or 60/82 days (long term) postinjection. Where indicated, BrdU (0.8 mg/ml) was given in drinking water 1 day before the first tamoxifen injection and kept until the end of the experiment. The pancreas was excised, processed, and stained as described in the Supplemental Experimental Procedures.

IF and Immunohistochemistry Staining

Rhodamine-DBA (Sigma) was used to detect ductal cells by confocal microscopy. IF and immunohistochemistry staining was performed as described elsewhere (Sancho et al., 2010). Antibodies are listed in the Supplemental Experimental Procedures. Quantification of the insulin-positive area in Ngn3 conditional transgenic mouse pancreas was performed on NanoZoomer 2.0-HT (HAMAMATSU) scanned slides using AdobePS-CS5.

Western Blot Analysis

Pancreas lysates were homogenized in RIPA lysis buffer supplemented with protease inhibitor (Sigma). 293T cells were lysed in NP-40 lysis buffer. Immunoblots were carried out as described elsewhere (Nateri et al., 2005). Antibodies are listed in the Supplemental Experimental Procedures.

Immunoprecipitations

Human embryonic kidney 293T (HEK293T) cells coexpressing HA-Ngn3 and Fbw7-Flag were treated for 5 hr with proteasome inhibitor MG-132 (25 μM; Calbiochem), lysed with 0.2% NP40 buffer, and incubated with anti-Flag or anti-HA agarose beads (Sigma). For the endogenous Fbw7-Ngn3 interaction assay, Ngn3 was immunoprecipitated from HCT116-*Fbw7*^{wt} and HCT116-*Fbw7*$^{\Delta}$ cells transfected with Ngn3-AA. Endogenous Fbw7 in inputs and immunoprecipitation (IP) samples was detected using anti-Fbw7 antibody (Bethyl Laboratories).

Ubiquitination Assays

For in vivo ubiquitination assays, His-Ub was affinity purified with nickel-nitrilotriacetic acid (NTA)-agarose beads, as described elsewhere (Davies et al., 2010). In vitro ubiquitination assays with Fbw7 and Fbw7α-ΔFbox-Flag immunoprecipitated complexes were performed as described elsewhere (Popov et al., 2007).

Fluorescence-Activated Cell Sorting Analysis

Single pancreatic cell suspensions were obtained by 30 min digestion in 1.6 mg/ml collagenase type IV (Whorttington), followed by filtration on a 70 μm nylon mesh. Cells from six age-matched (6- to 8-week-old) mice per genotype were sorted for GFP expression for each independent experiment.

DNA Isolation and Allele Recombination PCR

Genomic DNA from GFP+/GFP− cells sorted from six tamoxifen-injected *CFY* and *CY* mice was isolated by digestion in DirectPCR Lysis Reagent (Viagen). PCR primers used to detect the efficiency of recombination of *Fbw7* and *R26* alleles are given in the Supplemental Experimental Procedures.

Figure 6. *Fbw7* Deletion in the Adult Pancreatic Ducts Induces Direct Conversion of Ductal Cells into β Cells with No Intermediate Cell Division

(A) Scheme of the *CY* and *CFY* mouse model genotypes.
(B) Schematic diagram of *CY* pancreas before and after tamoxifen injection.
(C) PCR analysis of the *Fbw7* and *R26* loci on genomic DNA isolated from GFP-sorted *CY* and *CFY* cells 13 days post-tamoxifen injection. wt, *Fbw7* WT allele; flox, *Fbw7*^{f} unrecombined allele; Δ, *Fbw7* recombined allele; R26-LSL, *R26* unrecombined allele; R26-Δ, *R26* recombined allele.
(D) qPCR analysis of *Fbw7* mRNA in GFP+ (duct) and GFP− (endocrine and acinar) cells sorted from tamoxifen-injected *CFY* and *CY* mice (n = 6 pooled pancreas each) and GFP+ (β) cells from *MIP-GFP* mice (n = 3 pooled pancreas). n = 3 independent experiments.
(E and F) Quantification of number of ducts (E) or islets (F) per square millimeter in at least seven fields per mouse (representative example in adjacent picture); scale bar, 20 μm; n = 3 mice/genotype. ns, not significant.
(G) Quantification of the percentage of total ductal cells that are insulin positive in tamoxifen-injected *CY* (n = 10 mice/10,070 cells) and *CFY* mice (n = 7 mice/12,220 cells). Representative example in adjacent picture; scale bar, 20 μm.
(H–J) Triple IF for GFP, insulin (ins), and BrdU in tamoxifen-injected *CY* (H) or *CFY* (I and J) mice (5 days post-tamoxifen injection; n > 5 mice/genotype; representative picture shown). Nuclei were counterstained with DAPI. White dashed square (I) represents the area magnified (J). Error bars in (D)–(G) indicate SEM.
See also Figure S4 and Table S1.

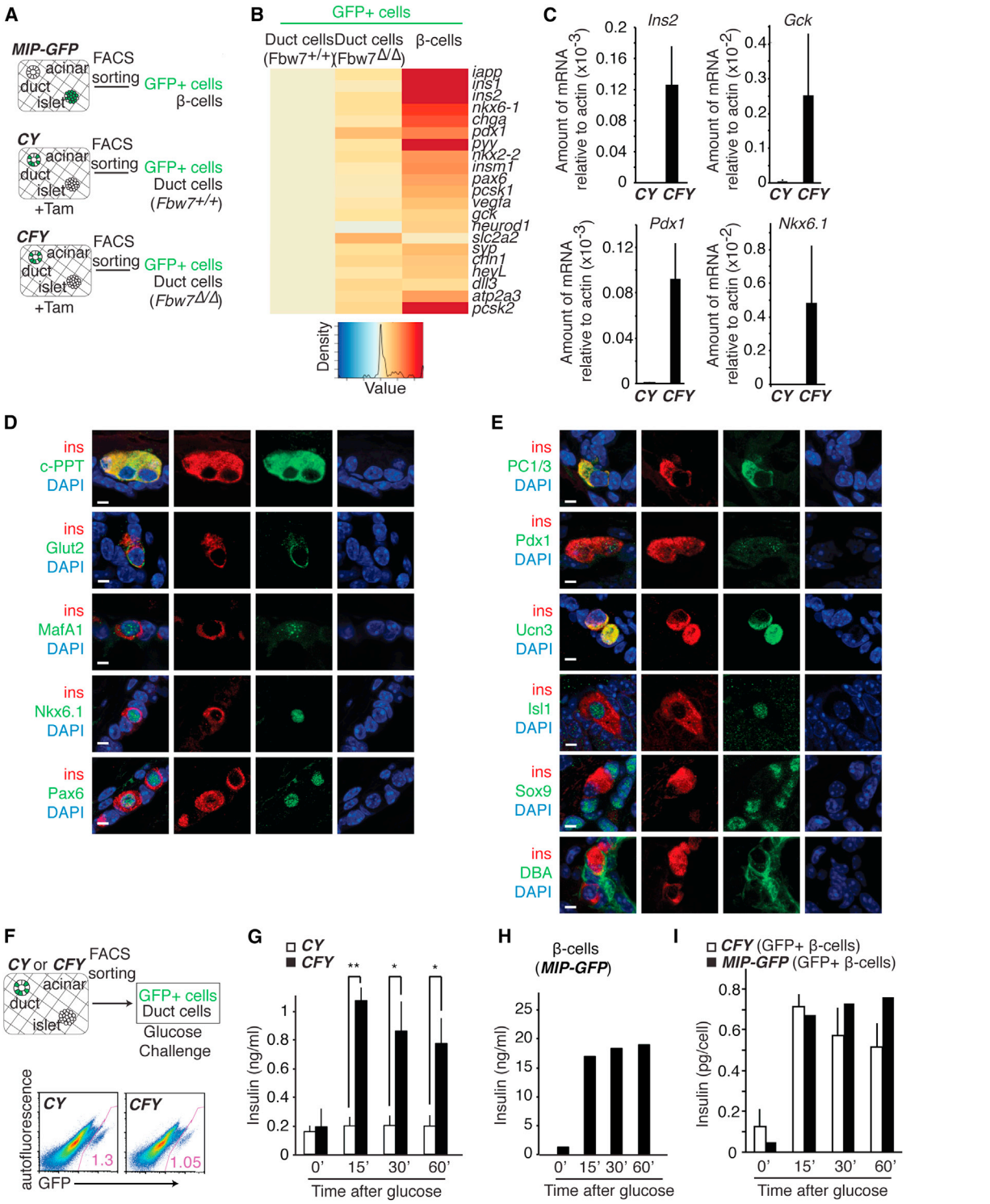

Figure 7. Converted β Cells Induced by *Fbw7* Deletion Resemble Functional Mature β Cells

(A) Schematic diagram of the comparison strategy used for the mRNA expression profile.

(B) Heat map representing expression of 15 β cell markers and 15 Ngn3 target genes in GFP+ sorted cells from tamoxifen-injected *CY* (n = 6), *CFY* (n = 6), and *MIP-GFP* (n = 3) mice.

(C) qPCR analysis of *Ins2*, *Gck*, *Pdx1*, and *Nkx6.1* expression in GFP+ cells sorted from *CY* and *CFY* mice (n = 6 pooled pancreas per genotype). n = 2 independent experiments.

(D and E) Double IF of insulin (ins) together with different β cell markers or ductal markers (Sox9, Dolichos biflorus agglutinin) in ductal *CFY* β cells. Scale bars, 5 μm. n > 5 mice per genotype (representative picture shown).

(legend continued on next page)

Microarray Analysis and qPCR

RNA was isolated from sorted GFP+ cells from tamoxifen-injected *CY* and *CFY* mice (six pooled pancreas per genotype) or *MIP-GFP* mice (three pooled pancreas) using a RNeasy Micro Kit (QIAGEN). RNA microarray hybridizations were performed by the Cancer Research UK Manchester Institute Microarray Service using the GeneChip Mouse Gene 1.0 ST array (Affymetrix) after genome amplification of the RNA.

For qPCR analysis of sorted cells, RNA was isolated as described for the microarray, and cDNA amplification was performed using the Quantitect whole transcriptome amplification kit (QIAGEN). For qPCR analysis in *Pdx1-Cre; Fbw7$^{f/f}$* mice, RNA was isolated using the RNeasy Mini Kit (QIAGEN), and cDNA was generated using the Transcriptor First Strand cDNA Synthesis Kit (Roche). Diluted cDNAs were used for qPCR SYBR-Green detection of target genes, using primer sequences given in the Supplemental Experimental Procedures.

Glucose Challenge In Vitro

Determination of insulin release after glucose challenge was performed as described elsewhere (Banga et al., 2012), with minor modifications. Briefly, 30,000 GFP+ sorted *CY* or *CFY* cells (from six pooled pancreas per genotype) or 5,000 GFP+ cells from *MIP-GFP* pancreas were plated per well in Dulbecco's modified Eagle's medium without serum/glucose/phenol red. Cells were starved for 2 hr, the medium was changed, and 20 mM glucose was added (final volume, 200 μl). Insulin concentration was determined in supernatants using the Mouse Insulin ELISA Kit (Crystal Chem).

Statistics

Statistical evaluation was performed using the Student's unpaired t test. *$p \leq 0.05$, **$p \leq 0.01$, ***$p \leq 0.001$ were considered statistically significant. See Table S1 for exact p values.

ACCESSION NUMBERS

The Gene Expression Omnibus accession number for the microarray data reported in Figure 7B is GSE58969.

SUPPLEMENTAL INFORMATION

Supplemental Information includes Supplemental Experimental Procedures, six figures, and one table and can be found with this article online at http://dx.doi.org/10.1016/j.stem.2014.06.019.

ACKNOWLEDGMENTS

We are grateful to the London Research Institute Animal Unit, Equipment Park, FACS facility; Bradley Spencer-Dene and Emma Nye in the Experimental Histopathology lab; and Richard Mitter in the Bioinformatics facility for technical help. We thank Hamamatsu for allowing us to perform the full slide scans using their NanoZoomer 2.0-HT. We thank D. Tuveson for *Pdx1-Cre* mice; J.J. Haigh for providing the pRosa26-DV1 vector used for generating the Ngn3-AA conditional transgenic mouse; and Nikita Popov and Bruce Clurman for providing reagents. We thank Stephen Pollard, Taija Makinen, and Ilaria Malanchi for critical reading of the manuscript. R.S. was funded by Marie Curie (MEIF-CT-2006-041119), MRC (G0901677), and ERC (281661) grants. R.G. was supported by an EMBO long-term fellowship. A.B. and R.S. are listed as inventors on an International Patent Application based on this work. The London Research Institute is funded by Cancer Research UK.

Received: August 21, 2013
Revised: April 11, 2014
Accepted: June 26, 2014
Published: August 7, 2014

REFERENCES

Al-Hasani, K., Pfeifer, A., Courtney, M., Ben-Othman, N., Gjernes, E., Vieira, A., Druelle, N., Avolio, F., Ravassard, P., Leuckx, G., et al. (2013). Adult duct-lining cells can reprogram into β-like cells able to counter repeated cycles of toxin-induced diabetes. Dev. Cell *26*, 86–100.

Apelqvist, A., Li, H., Sommer, L., Beatus, P., Anderson, D.J., Honjo, T., Hrabe de Angelis, M., Lendahl, U., and Edlund, H. (1999). Notch signalling controls pancreatic cell differentiation. Nature *400*, 877–881.

Atkinson, M.A., Bluestone, J.A., Eisenbarth, G.S., Hebrok, M., Herold, K.C., Accili, D., Pietropaolo, M., Arvan, P.R., Von Herrath, M., Markel, D.S., and Rhodes, C.J. (2011). How does type 1 diabetes develop?: the notion of homicide or β-cell suicide revisited. Diabetes *60*, 1370–1379.

Baeyens, L., Bonné, S., German, M.S., Ravassard, P., Heimberg, H., and Bouwens, L. (2006). Ngn3 expression during postnatal in vitro beta cell neogenesis induced by the JAK/STAT pathway. Cell Death Differ. *13*, 1892–1899.

Baeyens, L., Lemper, M., Leuckx, G., De Groef, S., Bonfanti, P., Stangé, G., Shemer, R., Nord, C., Scheel, D.W., Pan, F.C., et al. (2014). Transient cytokine treatment induces acinar cell reprogramming and regenerates functional beta cell mass in diabetic mice. Nat. Biotechnol. *32*, 76–83.

Banga, A., Akinci, E., Greder, L.V., Dutton, J.R., and Slack, J.M. (2012). In vivo reprogramming of Sox9+ cells in the liver to insulin-secreting ducts. Proc. Natl. Acad. Sci. USA *109*, 15336–15341.

Bonner-Weir, S., Toschi, E., Inada, A., Reitz, P., Fonseca, S.Y., Aye, T., and Sharma, A. (2004). The pancreatic ductal epithelium serves as a potential pool of progenitor cells. Pediatr. Diabetes *5* (*Suppl 2*), 16–22.

Bonner-Weir, S., Inada, A., Yatoh, S., Li, W.-C., Aye, T., Toschi, E., and Sharma, A. (2008). Transdifferentiation of pancreatic ductal cells to endocrine beta-cells. Biochem. Soc. Trans. *36*, 353–356.

Collombat, P., Xu, X., Ravassard, P., Sosa-Pineda, B., Dussaud, S., Billestrup, N., Madsen, O.D., Serup, P., Heimberg, H., and Mansouri, A. (2009). The ectopic expression of Pax4 in the mouse pancreas converts progenitor cells into alpha and subsequently beta cells. Cell *138*, 449–462.

Criscimanna, A., Speicher, J.A., Houshmand, G., Shiota, C., Prasadan, K., Ji, B., Logsdon, C.D., Gittes, G.K., and Esni, F. (2011). Duct cells contribute to regeneration of endocrine and acinar cells following pancreatic damage in adult mice. Gastroenterology *141*, 1451–1462, 1462.e1–1462.e1456.

Davies, C.C., Chakraborty, A., Cipriani, F., Haigh, K., Haigh, J.J., and Behrens, A. (2010). Identification of a co-activator that links growth factor signalling to c-Jun/AP-1 activation. Nat. Cell Biol. *12*, 963–972.

De Krijger, R.R., Aanstoot, H.J., Kranenburg, G., Reinhard, M., Visser, W.J., and Bruining, G.J. (1992). The midgestational human fetal pancreas contains cells coexpressing islet hormones. Dev. Biol. *153*, 368–375.

Dor, Y., Brown, J., Martinez, O.I., and Melton, D.A. (2004). Adult pancreatic beta-cells are formed by self-duplication rather than stem-cell differentiation. Nature *429*, 41–46.

Edlund, H. (2002). Pancreatic organogenesis—developmental mechanisms and implications for therapy. Nat. Rev. Genet. *3*, 524–532.

(F) Schematic diagram of the glucose challenge experiment design and fluorescence-activated cell sorting (FACS) profile indicating the sorting gate used for the isolation of 30,000 GFP+ cells (*CY*, *CFY*: n = 6 pooled pancreas) or 5,000 GFP+ cells (*MIP-GFP*: n = 3 pooled pancreas).
(G and H) Secreted insulin levels measured by ELISA from 30,000 GFP+ *CY*, *CFY* (G) and 5,000 *MIP-GFP* (H) cells 0–60 min after the addition of 20 mM glucose. n = 3 independent experiments.
(I) Insulin secretion per β cell is equivalent in *CFY* duct-derived and *MIP-GFP* islet cells, based on 300 converted β cells per well in the experiment in (G) and 5,000 β cells per well in the experiment in (H). Error bars in (C), (G), and (I) indicate SEM.
See also Figures S5 and S6 and Table S1.

Ejarque, M., Cervantes, S., Pujadas, G., Tutusaus, A., Sanchez, L., and Gasa, R. (2013). Neurogenin3 cooperates with Foxa2 to autoactivate its own expression. J. Biol. Chem. *288*, 11705–11717.

Esni, F., Ghosh, B., Biankin, A.V., Lin, J.W., Albert, M.A., Yu, X., MacDonald, R.J., Civin, C.I., Real, F.X., Pack, M.A., et al. (2004). Notch inhibits Ptf1 function and acinar cell differentiation in developing mouse and zebrafish pancreas. Development *131*, 4213–4224.

Fujikura, J., Hosoda, K., Iwakura, H., Tomita, T., Noguchi, M., Masuzaki, H., Tanigaki, K., Yabe, D., Honjo, T., and Nakao, K. (2006). Notch/Rbp-j signaling prevents premature endocrine and ductal cell differentiation in the pancreas. Cell Metab. *3*, 59–65.

Gradwohl, G., Dierich, A., LeMeur, M., and Guillemot, F. (2000). neurogenin3 is required for the development of the four endocrine cell lineages of the pancreas. Proc. Natl. Acad. Sci. USA *97*, 1607–1611.

Grim, J.E., Gustafson, M.P., Hirata, R.K., Hagar, A.C., Swanger, J., Welcker, M., Hwang, H.C., Ericsson, J., Russell, D.W., and Clurman, B.E. (2008). Isoform- and cell cycle-dependent substrate degradation by the Fbw7 ubiquitin ligase. J. Cell Biol. *181*, 913–920.

Habener, J.F., Kemp, D.M., and Thomas, M.K. (2005). Minireview: transcriptional regulation in pancreatic development. Endocrinology *146*, 1025–1034.

Hara, M., Wang, X., Kawamura, T., Bindokas, V.P., Dizon, R.F., Alcoser, S.Y., Magnuson, M.A., and Bell, G.I. (2003). Transgenic mice with green fluorescent protein-labeled pancreatic beta -cells. Am. J. Physiol. Endocrinol. Metab. *284*, E177–E183.

Heremans, Y., Van De Casteele, M., in't Veld, P., Gradwohl, G., Serup, P., Madsen, O., Pipeleers, D., and Heimberg, H. (2002). Recapitulation of embryonic neuroendocrine differentiation in adult human pancreatic duct cells expressing neurogenin 3. J. Cell Biol. *159*, 303–312.

Hingorani, S.R., Petricoin, E.F., Maitra, A., Rajapakse, V., King, C., Jacobetz, M.A., Ross, S., Conrads, T.P., Veenstra, T.D., Hitt, B.A., et al. (2003). Preinvasive and invasive ductal pancreatic cancer and its early detection in the mouse. Cancer Cell *4*, 437–450.

Hoeck, J.D., Jandke, A., Blake, S.M., Nye, E., Spencer-Dene, B., Brandner, S., and Behrens, A. (2010). Fbw7 controls neural stem cell differentiation and progenitor apoptosis via Notch and c-Jun. Nat. Neurosci. *13*, 1365–1372.

Inada, A., Nienaber, C., Katsuta, H., Fujitani, Y., Levine, J., Morita, R., Sharma, A., and Bonner-Weir, S. (2008). Carbonic anhydrase II-positive pancreatic cells are progenitors for both endocrine and exocrine pancreas after birth. Proc. Natl. Acad. Sci. USA *105*, 19915–19919.

Iriuchishima, H., Takubo, K., Matsuoka, S., Onoyama, I., Nakayama, K.I., Nojima, Y., and Suda, T. (2011). Ex vivo maintenance of hematopoietic stem cells by quiescence induction through Fbxw7 overexpression. Blood *117*, 2373–2377.

Ishikawa, Y., Onoyama, I., Nakayama, K.I., and Nakayama, K. (2008). Notch-dependent cell cycle arrest and apoptosis in mouse embryonic fibroblasts lacking Fbxw7. Oncogene *27*, 6164–6174.

Jandke, A., Da Costa, C., Sancho, R., Nye, E., Spencer-Dene, B., and Behrens, A. (2011). The F-box protein Fbw7 is required for cerebellar development. Dev. Biol. *358*, 201–212.

Jensen, J., Pedersen, E.E., Galante, P., Hald, J., Heller, R.S., Ishibashi, M., Kageyama, R., Guillemot, F., Serup, P., and Madsen, O.D. (2000). Control of endodermal endocrine development by Hes-1. Nat. Genet. *24*, 36–44.

Lysy, P.A., Weir, G.C., and Bonner-Weir, S. (2012). Concise review: pancreas regeneration: recent advances and perspectives. Stem Cells Transl. Med. *1*, 150–159.

Matsumoto, A., Onoyama, I., Sunabori, T., Kageyama, R., Okano, H., and Nakayama, K.I. (2011). Fbxw7-dependent degradation of Notch is required for control of "stemness" and neuronal-glial differentiation in neural stem cells. J. Biol. Chem. *286*, 13754–13764.

Means, A.L., Xu, Y., Ray, K.C., and Gu, G. (2008). A CK19(CreERT) knockin mouse line allows for conditional DNA recombination in epithelial cells in multiple endodermal organs. Genesis *46*, 318–323.

Murtaugh, L.C., Stanger, B.Z., Kwan, K.M., and Melton, D.A. (2003). Notch signaling controls multiple steps of pancreatic differentiation. Proc. Natl. Acad. Sci. USA *100*, 14920–14925.

Nakayama, K.I., and Nakayama, K. (2006). Ubiquitin ligases: cell-cycle control and cancer. Nat. Rev. Cancer *6*, 369–381.

Nateri, A.S., Spencer-Dene, B., and Behrens, A. (2005). Interaction of phosphorylated c-Jun with TCF4 regulates intestinal cancer development. Nature *437*, 281–285.

Nyabi, O., Naessens, M., Haigh, K., Gembarska, A., Goossens, S., Maetens, M., De Clercq, S., Drogat, B., Haenebalcke, L., Bartunkova, S., et al. (2009). Efficient mouse transgenesis using Gateway-compatible ROSA26 locus targeting vectors and F1 hybrid ES cells. Nucleic Acids Res. *37*, e55.

Oka, C., Nakano, T., Wakeham, A., de la Pompa, J.L., Mori, C., Sakai, T., Okazaki, S., Kawaichi, M., Shiota, K., Mak, T.W., and Honjo, T. (1995). Disruption of the mouse RBP-J kappa gene results in early embryonic death. Development *121*, 3291–3301.

Oliver-Krasinski, J.M., and Stoffers, D.A. (2008). On the origin of the beta cell. Genes Dev. *22*, 1998–2021.

Onoyama, I., Tsunematsu, R., Matsumoto, A., Kimura, T., de Alborán, I.M., Nakayama, K., and Nakayama, K.I. (2007). Conditional inactivation of Fbxw7 impairs cell-cycle exit during T cell differentiation and results in lymphomatogenesis. J. Exp. Med. *204*, 2875–2888.

Onoyama, I., Suzuki, A., Matsumoto, A., Tomita, K., Katagiri, H., Oike, Y., Nakayama, K., and Nakayama, K.I. (2011). Fbxw7 regulates lipid metabolism and cell fate decisions in the mouse liver. J. Clin. Invest. *121*, 342–354.

Pagliuca, F.W., and Melton, D.A. (2013). How to make a functional β-cell. Development *140*, 2472–2483.

Piper, K., Brickwood, S., Turnpenny, L.W., Cameron, I.T., Ball, S.G., Wilson, D.I., and Hanley, N.A. (2004). Beta cell differentiation during early human pancreas development. J. Endocrinol. *181*, 11–23.

Popov, N., Wanzel, M., Madiredjo, M., Zhang, D., Beijersbergen, R., Bernards, R., Moll, R., Elledge, S.J., and Eilers, M. (2007). The ubiquitin-specific protease USP28 is required for MYC stability. Nat. Cell Biol. *9*, 765–774.

Roark, R., Itzhaki, L., and Philpott, A. (2012). Complex regulation controls Neurogenin3 proteolysis. Biol. Open *1*, 1264–1272.

Sancho, R., Jandke, A., Davis, H., Diefenbacher, M.E., Tomlinson, I., and Behrens, A. (2010). F-box and WD repeat domain-containing 7 regulates intestinal cell lineage commitment and is a haploinsufficient tumor suppressor. Gastroenterology *139*, 929–941.

Sancho, R., Blake, S.M., Tendeng, C., Clurman, B.E., Lewis, J., and Behrens, A. (2013). Fbw7 repression by hes5 creates a feedback loop that modulates Notch-mediated intestinal and neural stem cell fate decisions. PLoS Biol. *11*, e1001586.

Schwitzgebel, V.M., Scheel, D.W., Conners, J.R., Kalamaras, J., Lee, J.E., Anderson, D.J., Sussel, L., Johnson, J.D., and German, M.S. (2000). Expression of neurogenin3 reveals an islet cell precursor population in the pancreas. Development *127*, 3533–3542.

Srinivas, S., Watanabe, T., Lin, C.S., William, C.M., Tanabe, Y., Jessell, T.M., and Costantini, F. (2001). Cre reporter strains produced by targeted insertion of EYFP and ECFP into the ROSA26 locus. BMC Dev. Biol. *1*, 4.

Swales, N., Martens, G.A., Bonné, S., Heremans, Y., Borup, R., Van de Casteele, M., Ling, Z., Pipeleers, D., Ravassard, P., Nielsen, F., et al. (2012). Plasticity of adult human pancreatic duct cells by neurogenin3-mediated reprogramming. PLoS ONE *7*, e37055.

Teta, M., Long, S.Y., Wartschow, L.M., Rankin, M.M., and Kushner, J.A. (2005). Very slow turnover of beta-cells in aged adult mice. Diabetes *54*, 2557–2567.

Thompson, B.J., Jankovic, V., Gao, J., Buonamici, S., Vest, A., Lee, J.M., Zavadil, J., Nimer, S.D., and Aifantis, I. (2008). Control of hematopoietic stem cell quiescence by the E3 ubiquitin ligase Fbw7. J. Exp. Med. *205*, 1395–1408.

Van de Casteele, M., Leuckx, G., Baeyens, L., Cai, Y., Yuchi, Y., Coppens, V., De Groef, S., Eriksson, M., Svensson, C., Ahlgren, U., et al. (2013). Neurogenin

3+ cells contribute to β-cell neogenesis and proliferation in injured adult mouse pancreas. Cell Death Dis. *4*, e523.

Ventura, A., Kirsch, D.G., McLaughlin, M.E., Tuveson, D.A., Grimm, J., Lintault, L., Newman, J., Reczek, E.E., Weissleder, R., and Jacks, T. (2007). Restoration of p53 function leads to tumour regression in vivo. Nature *445*, 661–665.

Wang, S., Hecksher-Sorensen, J., Xu, Y., Zhao, A., Dor, Y., Rosenberg, L., Serup, P., and Gu, G. (2008). Myt1 and Ngn3 form a feed-forward expression loop to promote endocrine islet cell differentiation. Dev. Biol. *317*, 531–540.

Wang, Z., Inuzuka, H., Fukushima, H., Wan, L., Gao, D., Shaik, S., Sarkar, F.H., and Wei, W. (2012). Emerging roles of the FBW7 tumour suppressor in stem cell differentiation. EMBO Rep. *13*, 36–43.

Welcker, M., and Clurman, B.E. (2008). FBW7 ubiquitin ligase: a tumour suppressor at the crossroads of cell division, growth and differentiation. Nat. Rev. Cancer *8*, 83–93.

Welcker, M., Orian, A., Jin, J., Grim, J.E., Harper, J.W., Eisenman, R.N., and Clurman, B.E. (2004). The Fbw7 tumor suppressor regulates glycogen synthase kinase 3 phosphorylation-dependent c-Myc protein degradation. Proc. Natl. Acad. Sci. USA *101*, 9085–9090.

Xu, X., D'Hoker, J., Stangé, G., Bonné, S., De Leu, N., Xiao, X., Van de Casteele, M., Mellitzer, G., Ling, Z., Pipeleers, D., et al. (2008). Beta cells can be generated from endogenous progenitors in injured adult mouse pancreas. Cell *132*, 197–207.

Yi, P., Park, J.S., and Melton, D.A. (2013). Betatrophin: a hormone that controls pancreatic β cell proliferation. Cell *153*, 747–758.

Zaret, K.S. (2008). Genetic programming of liver and pancreas progenitors: lessons for stem-cell differentiation. Nat. Rev. Genet. *9*, 329–340.

Zhou, Q., Brown, J., Kanarek, A., Rajagopal, J., and Melton, D.A. (2008). In vivo reprogramming of adult pancreatic exocrine cells to beta-cells. Nature *455*, 627–632.